JOURNAL OF VIROLOGY, Sept. 2000, p. 7972–7979 Vol. 74, No. 17
0022-538X/00/$04.00+0

In Vitro and In Vivo Infection of Neural Cells by a Recombinant Measles Virus Expressing Enhanced Green Fluorescent Protein

W. PAUL DUPREX,[1]* STEPHEN McQUAID,[2] BRANKA ROSCIC-MRKIC,[3] ROBERTO CATTANEO,[4] CECILIA McCALLISTER,[1] AND BERT K. RIMA[1]

School of Biology and Biochemistry, The Queen's University of Belfast, Belfast BT9 7BL,[1] and Neuropathology Laboratory, Royal Group of Hospitals Trust, Belfast BT12 6B1,[2] Northern Ireland, United Kingdom; Molecular Medicine Program, Mayo Clinic, Rochester, Minnesota 55905[4]; and Institut für Molekularbiologie, Universität Zürich, CH-8057 Zürich, Switzerland[3]

Received 9 February 2000/Accepted 31 May 2000

This study focused on the in vitro infection of mouse and human neuroblastoma cells and the in vivo infection of the murine central nervous system with a recombinant measles virus. An undifferentiated mouse neuroblastoma cell line (TMN) was infected with the vaccine strain of measles virus (MVeGFP), which expresses enhanced green fluorescent protein (EGFP). MVeGFP infected the cells, and cell-to-cell spread was studied by virtue of the resulting EGFP autofluorescence, using real-time confocal microscopy. Cells were differentiated to a neuronal phenotype, and extended processes, which interconnected the cells, were observed. It was also possible to infect the differentiated neuroblastoma cells (dTMN) with MVeGFP. Single autofluorescent EGFP-positive cells were selected at the earliest possible point in the infection, and the spread of EGFP autofluorescence was monitored. In this instance the virus used the interconnecting processes to spread from cell to cell. Human neuroblastoma cells (SH-SY-5Y) were also infected with MVeGFP. The virus infected these cells, and existing processes were used to initiate new foci of infection at distinct regions of the monolayer. Transgenic animals expressing CD46, a measles virus receptor, and lacking interferon type 1 receptor gene were infected intracerebrally with MVeGFP. A productive infection ensued, and the mice exhibited clinical signs of infection, such as ataxia and an awkward gait, identical to those previously observed for the parental virus (Edtag). Mice were sacrificed, and brain sections were examined for EGFP autofluorescence by confocal scanning laser microscopy over a period of 6 h. EGFP was detected in discrete focal regions of the brain and in processes, which extended deep into the parenchyma. Collectively, these results indicate (i) that MVeGFP can be used to monitor virus replication sensitively, in real time, in animal tissues, (ii) that infection of ependymal cells and neuroblasts provides a route by which measles virus can enter the central nervous system in mouse models of encephalitis, and (iii) that upon infection, the virus spreads transneuronally.

Measles virus (MV) infects over 40 million individuals each year. Encephalomyelitis can occur as part of the acute infection, while subacute sclerosing panencephalitis (SSPE) and measles inclusion body encephalitis (MIBE) are two rare sequelae of central nervous system (CNS) infections (1, 42). SSPE is invariably fatal and occurs an average of 8 years after the acute infection. There is no evidence to suggest that a variant virus is involved in the primary infection, nor has any vaccine virus has been implicated in the establishment of SSPE. The virus appears to persist in the body at an unknown site (37). In SSPE, CNS infection develops in the presence of high titers of antiviral antibodies, and the isolated viruses are defective in budding (12). Mutations accumulate in the virus genome, especially in the fusion and matrix genes, and transcription of envelope genes is reduced by an altered transcription gradient (3, 8, 41, 43). MIBE is observed in immunosupressed patients, for example, in some of those with human immunodeficiency virus type 1 infection and those undergoing immunosuppressive therapy. It has become more prevalent in recent years and leads to the death of the individual within a few weeks.

Two approaches have been used to study MV neurotropism in efforts to generate a small-animal model for CNS infection. First, following the identification of the complement cofactor CD46 as a receptor for the Edmonston strain of MV (11, 30) a number of groups have produced transgenic animals which express the receptor (6, 16, 28, 29, 32, 34). The inflammatory response in the CNS of transgenic animals has been investigated. $CD4^+$ and $CD8^+$ T lymphocytes, B lymphocytes, and macrophages were observed to infiltrate the brain parenchyma, major histocompatibility complex class I and class II molecules were upregulated, and the abundance of certain chemokine mRNAs increased. Apoptosis of neurons was also observed (25). The role of the immune system in the protection of $CD46^+$ mice from MV-induced encephalitis has also been examined in this transgenic model (21). Immature mice and immunologically compromised immature and adult mice were shown to be susceptible to neurological disease. Immunocompetent adult mice were efficiently protected from virus infection, indicating that lymphocytes have an important role in disease progression. A second approach has been to isolate rodent brain-adapted strains of MV by repeated passage in the CNS (10, 20, 23, 24, 35). The majority of sequence alterations in these strains reside in the H gene (38), and it is possible that these changes allow MV to infect rodent neural cells using a different receptor. We have recently demonstrated, using the MV rescue system (33), that the H gene is sufficient to permit the transfer of neurovirulence determinants from a rodent brain-adapted strain to a nonneurovirulent vaccine strain (13).

The precise mechanism of MV spread in the CNS is unknown, although it has been suggested that the virus spreads

* Corresponding author: Mailing address: School of Biology and Biochemistry, The Queen's University of Belfast, Medical Biology Centre, 97 Lisburn Rd., Belfast BT9 7BL, Northern Ireland, United Kingdom. Phone: 44-28-90272060. Fax: 44-28-90236505. E-mail: p.duprex@qub.ac.uk.

transneuronally (2, 22, 32, 46). We have recently used a recombinant MV which expresses enhanced green fluorescent protein (EGFP) (19) to infect human astrocytoma cells and observed spread from cell to cell via the interconnecting astrocytic process (14). The recombinant virus, MVeGFP, is based on the Edmonston vaccine strain. This strain is nonneurovirulent in the rodent model of MV encephalitis, in which suckling C57/BL/6 mice are infected intracerebrally with 200 50% tissue culture infective doses ($TCID_{50}$) of virus. Recently a transgenic mouse ($Ifnar^{ko}$-CD46Ge) has been generated which expresses CD46 with human-like tissue specificity and contains a targeted mutation that inactivates the alpha/beta interferon receptor (28, 29). Intracerebral challenge of weanling mice (6 to 8 weeks old) with 3×10^3 or 10^5 PFU of Edmonston virus resulted in similar levels of mortality in these animals (approximately 90%). However, incubation times were prolonged in the mice infected with lower doses of virus. In this study we begin to address the unresolved question of how the virus might spread from cell to cell in the CNS and show, in an MV-rodent model of encephalitis, that virus-infected cells do not have the morphological characteristics of neurons. This is the first investigation that has indirectly observed MV in ex vivo brain tissue using a recombinant virus which expresses an autofluorescent protein. MVeGFP is therefore a useful virus which may substantially augment and enhance our understanding MV neuropathogenesis.

MATERIALS AND METHODS

Cells and virus. Vero cells were grown in Dulbecco's modified Eagle's medium (DMEM; Gibco) containing 8% newborn calf serum (NCS; Gibco) and penicillin-streptomycin (100 μg/ml). These were used routinely for the growth of MV, which was propagated in DMEM containing 2% NCS. Murine neuroblastoma cells (TMN) were obtained from Carvell Williams (The Queen's University of Belfast). TMN cells were grown in growth medium consisting of DMEM (64%), nutrient mixture Ham's F-12 with Glutamax (25%), minimal essential medium alpha (5%), supplemented with 1% fetal calf serum (FCS; Gibco), 4% NCS, and antibiotics as above. Human neuroblastoma cells (SH-SY-5Y) were obtained from Janet Johnston (The Queen's University of Belfast). SH-SY-5Y cells were grown in growth medium consisting of DMEM supplemented with 10% FCS and antibiotics as above. MVeGFP virus was rescued from a modified full-length infectious antigenomic clone of MV generated by Lars Hangartner (19) using the MV helper cell line 293-3-46, which was maintained as previously described (33). MVeGFP was propagated as described previously (14). Virus stocks were produced in Vero cells following plaque purification, and titers of approximately 5×10^5 $TCID_{50}$/ml were obtained. Fluorescence microscopy was used routinely to ascertain that EGFP expression was retained upon virus passage and to ensure that mutants which had lost the ability to express EGFP were present below the limit of detection. Titers were obtained by 50% endpoint dilution assays and are expressed as $TCID_{50}$, determined by the method of Reed and Muench (36).

Differentiation of TMN cells. TMN cells were differentiated over a period of 8 days using cyclic AMP (cAMP; Sigma) and 5′-bromo-2′-deoxyuridine (Sigma). Differentiation medium (TMN growth medium supplemented with 1 mM cAMP and 3.7 mM 5′-bromo-2′-deoxyuridine), was prepared freshly prior to differentiation and stored for no longer than 4 weeks at 4°C. TMN cells were seeded in 24-well plates (10^5 cells/well) in differentiation medium and incubated for 5 days at 37°C in 5% (vol/vol) CO_2. Cells were examined daily by phase contrast microscopy for the appearance of neurites. Fresh differentiation medium was then added, and the cells were incubated for a further 3 days. After this time, based on the resultant morphological changes, the TMN cells were considered to be differentiated.

Immunofluorescence and confocal microscopy. TMN cells were grown on glass coverslips to 80% confluency. Monolayers were rinsed with maintenance medium (DMEM [67%], nutrient mixture Ham's F-12 with Glutamax [25%], MEM alpha [5%], supplemented with 1% FCS, 1% NCS, and penicillin-streptomycin [100 μg/ml]). Cells were infected with MVeGFP at a multiplicity of infection (MOI) of 0.01 and incubated for 1 h at 37°C. After this time unadsorbed virus was removed, maintenance medium was added, and cells were incubated at 37°C. EGFP autofluorescence, observed by UV microscopy, was used to monitor the progress of MVeGFP infection. Cells were fixed for 10 min in 4% paraformaldehyde. Propidium iodide solution (6 μg/ml) was used to counterstain the nuclei. Cells on coverslips were incubated in propidium iodide solution for 5 s at room temperature. Unbound propidium iodide was removed by three rinses in phosphate-buffered saline. A Leica TCS/NT confocal microscope equipped with a krypton-argon laser as the source for the ion beam was used to examine the samples for fluorescence. EGFP was visualized by virtue of its autofluorescence by excitation at 488 nm with a 506-nm to 538-nm band-pass emission filter, and propidium iodide-stained samples were imaged by excitation at 568 nm with a 564-nm to 596-nm band-pass emission filter.

Vital fluorescent microscopy. Differentiated TMN (dTMN) cells cultured in 24-well trays were infected at an MOI of 0.01 with MVeGFP. SH-SY-5Y cells, grown to 80% confluency in 25-cm^2 tissue culture bottles, were infected at a similar MOI. An inverted UV microscope was used to monitor the monolayers for the appearance of EGFP autofluorescence, and single infected cells were identified. Bottles and trays were oriented on the microscope stage, which was marked to permit repeated observation of the chosen foci in the differentiated cells. Images of EGFP autofluorescent cells were collected by confocal scanning laser microscopy (CSLM) as previously described (14). Observations were made over a period of 90 h at intervals of between 4 and 8 h.

Infection of transgenic mice and observation of MVeGFP-infected cells ex vivo. Transgenic mice ($Ifnar^{ko}$-CD46Ge) contain the complete gene sequence and surrounding flanking regions of human CD46 and lack the interferon type 1 receptor gene (28). Four-day-old suckling $Ifnar^{ko}$CD46Ge mice were obtained from in-house breeding colonies in the Laboratory Service Unit, The Queen's University of Belfast. Animals were kept in a barrier system with light negative pressure and a 12-h day (artificial light). Mice were infected into the right cerebral hemisphere under mild halothane anesthesia with 200 $TCID_{50}$ of MVeGFP in a total volume of 20 μl. Negative control mice were injected with an equivalent volume of tissue culture medium. Mice were checked for clinical symptoms daily. At 3 days postinfection (d.p.i.), mice were sacrificed under narcosis. The whole brain was removed and placed in a petri dish containing Optimem (Gibco). Brains were sectioned sagittally, and the tissue was maintained at 37°C in 5% CO_2 for a period of 6 h. During this time, repeated observations were made of EGFP autofluorescent cells within the tissue using an inverted UV microscope. Image stacks (ca. 20 to 150 μm) were collected through relatively large sections of the tissue by CSLM. Brain tissues were kept in the same orientation throughout the observation period to permit reidentification of infectious centers.

Immunopathology and histology. MV was detected in 8-μm brain sections as previously described, using a monoclonal antibody which recognises the nucleocapsid protein (13, 26).

RESULTS

MVeGFP infection of murine neuroblastoma cells. In order to ascertain whether a derivative of the attenuated Edmonston vaccine strain of MV can infect TMN cells, undifferentiated TMN cells grown to a confluency of 80% were infected at an MOI of 0.01 with recombinant MVeGFP. Infected cells were located using phase contrast and UV microscopy. Fewer infected cells than expected were observed, based on the MOI used, indicating that the infection occurred relatively infrequently. Nevertheless, the infection spread from cell to cell by fusion, and syncytia were generated. Confocal microscopy was used to visualize EGFP autofluorescence, and Fig. 1A shows a representative focus of infection at 90 h postinfection (h.p.i.). Cells were fixed and permeabilized using paraformaldehyde, which has no effect on EGFP autofluorescence. Propidium iodide was used to counterstain the nuclei. The nuclei were large compared to the overall size of the cells. Remarkably, MVeGFP was observed to spread from cell to cell by fusion. The relatively large nuclei clustered in the center of syncytia. EGFP was dispersed throughout the cytoplasm of both single infected cells, observed earlier in the infection, and syncytia. Some accumulation of EGFP was observed in the nuclei of infected cells. This phenomenon has been noted previously in astrocytoma cells and is assumed, at present, to be nonspecific.

MVeGFP infection of differentiated TMN cells. In order to observe whether differentiation of TMN cells affected their ability to be infected by MVeGFP, TMN cells were differentiated for 8 days in the presence of 1 mM cAMP and 3.7 μM 5′-bromo-2′-deoxyuridine. The morphology of the cells was observed routinely by phase contrast microscopy throughout the procedure. At the outset a small proportion, approximately 0.5%, of the cells had extended processes. Many more projections, which were approximately the length of a single cell, were observed after 3 days. By this stage almost all of the cells possessed at least one process. Ramified processes, which increased in number throughout the differentiation procedure,

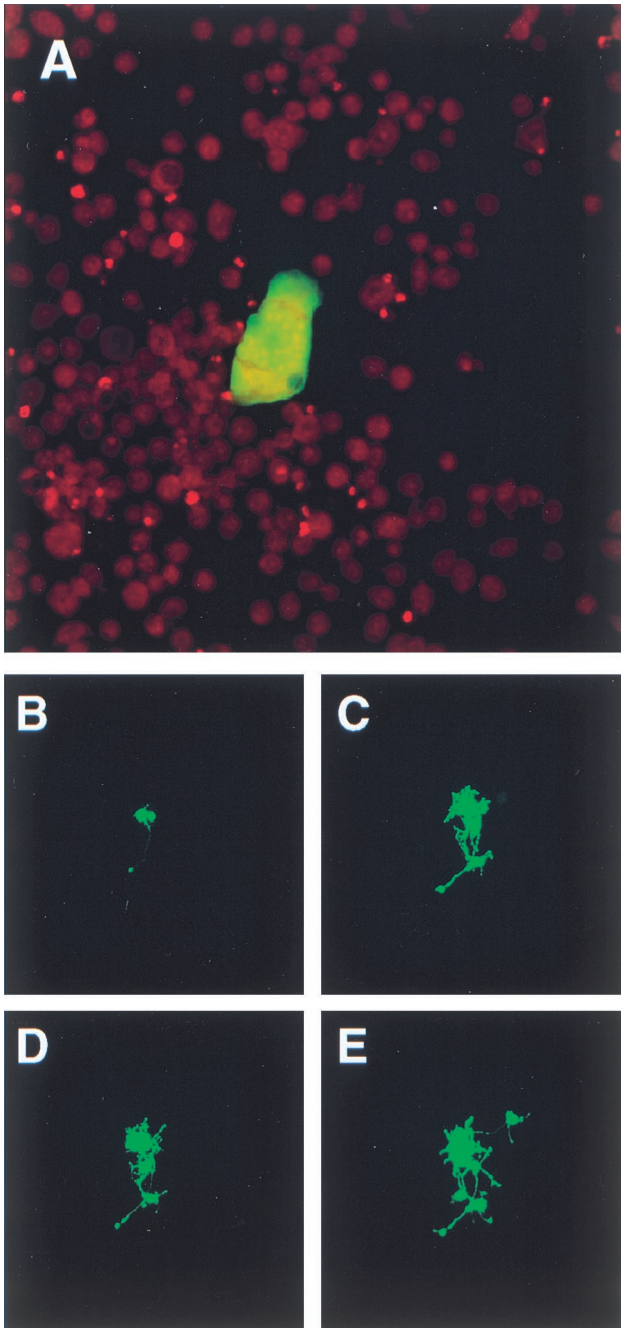

FIG. 1. Cell-to-cell spread of MVeGFP in undifferentiated and differentiated murine neuroblastoma cells. TMN cells at a confluency of 80% were infected with MVeGFP at an MOI of 0.01. Undifferentiated TMN cells were fixed and examined by CSLM for fluorescence. (A) Syncytium of infected undifferentiated TMN cells at 90 h.p.i. Nuclei were counterstained using propidium iodide, and micrographs represent a 10-μm composite optical section. Infected dTMN cells were identified by UV microscopy, and the positions of infectious centers were marked to aid in their reidentification throughout a time period of 42 h. (B) Two infected dTMN cells, one of which has an extended process (48 h.p.i.). (C) A number of newly infected cells with interconnecting autofluorescent processes (66 h.p.i.). (D) No additional fluorescent cells were observed by 72 h.p.i., but a number of additional autofluorescent processes were visible. By 90 h.p.i., further TMN cells became infected via these processes (E). Autofluorescent images (B to E) were collected as single optical sections by CSLM.

were seen to connect neighboring cells. Cell numbers did not increase over the 8 days. No significant numbers of additional neurites were observed to develop after this time period.

dTMN cells were infected at an MOI of 0.01 with MVeGFP. Cells were infectable, but only small numbers of EGFP-positive cells, approximately 1 in 1,000, were detected. Single MVeGFP-infected cells were observed by their autofluorescence at 40 h.p.i. A number of these infectious centers were located and marked to assist in their relocation over the time course. Cells were observed every 4 to 8 h. Representative images are shown in Fig. 1B to E at 48, 66, 72, and 90 h.p.i. In this instance, because the cells were observed in real time, the nuclei are unstained and therefore uninfected cells are not visible. EGFP autofluorescence was detected throughout the cell cytoplasm and accumulated in the nucleus. Phase contrast microscopy indicated that fusion occurred between infected cells (data not shown). Two infected cells are shown in Fig. 1B. A process, terminating in a bouton, extends from the infected cell on the left. When phase contrast microscopy was used to examine the uninfected cells, it was noted that this neurite seemed to interact intimately with a neighboring cell. Interestingly, this cell remained uninfected throughout the period of observation. By 66 h.p.i., two newly infected cells were observed along with a large number of interconnecting, ramified processes (Fig. 1C). At 72 h.p.i. the first two observed infected cells were fused; this was verified at higher magnifications using phase contrast microscopy, and further processes extended from the cell bodies (Fig. 1D). Uninfected cells surrounding this focus seemed to be in close contact with infected cells, as observed by phase contrast microscopy. Two more infected cells were observed at 90 h.p.i. (Fig. 1E). The upper outlying infected cell is clearly connected to the main body of infected cells by a process. At later time points, more of the interconnecting processes were observed to show EGFP autofluorescence. Cell-to-cell spread appears to occur rapidly, and cells in which EGFP influx occurred immediately at the site of fusion and spread from this site, increasing in intensity to fill the whole cell, were never observed. Rather, as in the case of the undifferentiated TMN cells, the nuclei were the first subcellular structures to exhibit EGFP autofluorescence.

MVeGFP infection of human neuroblastoma cells. SH-SY-5Y is a human neuroblastoma cell line which expresses well-characterized neuronal markers such as neurofilament protein (data not shown). Phase contrast microscopy indicated that some cells developed long neuronal processes, which were many times the length of single cells. We were therefore interested to ascertain if these processes could be used to permit MVeGFP to infect neighboring cells in a similar manner to the process-mediated spread observed previously in the dTMN cells. In order to determine if the recombinant, EGFP-expressing MV could infect the human neuroblastoma cell line SH-SY-5Y, cells were grown to 95% confluency and infected at an MOI of 0.01. Cells were infected at the level expected from the MOI, and EGFP autofluorescence was readily observed at 48 h.p.i. Due to the confluence of the cells, large syncytia were formed by 60 h.p.i. When processes were available, the virus was observed to utilize these to infect neighboring cells. A typical example is shown in Fig. 2. At 80 h.p.i. a long process was observed to extend from the large EGFP-positive syncytium, and a single cell is infected. The process traverses many uninfected, underlying SH-SY-5Y cells, and a number of boutons (arrowed) are visible along its length (Fig. 2A). Six hours later, a small syncytium was observed to develop from this single infected cell. During this time, the original syncytium has increased in size (Fig. 2B). As the outlying syncytium increased in size, the connecting process remained intact and brightly

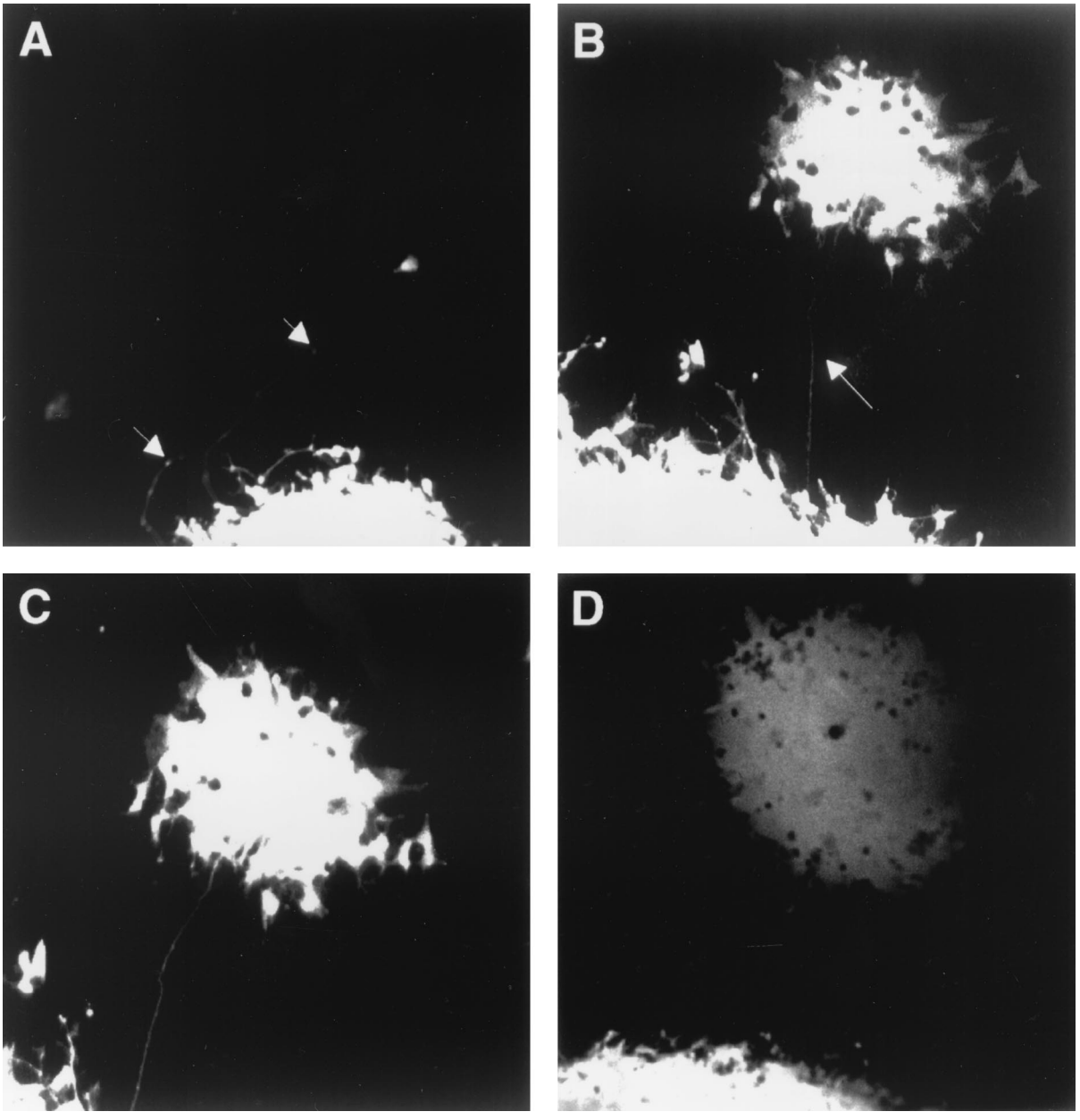

FIG. 2. Process-mediated cell-to-cell spread in human neuroblastoma cells infected with MVeGFP. SH-SY-5Y cells at a confluency of 95% were infected with MVeGFP at an MOI of 0.01. (A) Syncytium with a number of extended processes (arrows) was identified by UV microscopy (80 h.p.i.). A single infected cell is visible at the end of one of the processes. This infectious center was observed for a further 24 h. (B) By 86 h.p.i., a new syncytium had developed from the single infected cell. The connecting process remained visible and is indicated by an arrow. (C) By 87 h.p.i., the autofluorescence in a number of cells on the periphery of the secondary syncytium increased in intensity. (D) The two syncytia increased in size by 104 h.p.i. Autofluorescent images were collected as single optical sections by CSLM and are shown in "false" white.

autofluorescent (Fig. 2C). Both syncytia increased in size as time progressed, and other processes were observed to emanate from the edge of the syncytia at 104 h.p.i. (Fig. 2D). By this stage the secondary syncytium comprised approximately 100 infected cells.

Infection of CD46 transgenic animals. EGFP autofluorescence is a very sensitive indicator of MVeGFP infection in neuroblastoma cells. Having observed the cell-to-cell spread of MVeGFP in vitro, we tested if this virus would be useful for the in vivo observation of MV. Intracerebral injection into the CNS of neonatal rodents is the only animal model available which permits extensive exploration of MV neuropathogenesis. We therefore chose to use Ifnar^{ko}-CD46Ge transgenic animals to investigate whether MVeGFP could be detected by virtue of the EGFP autofluorescence in the CNS.

A litter of six 5-day-old Ifnar^{ko}-CD46Ge transgenic mice were infected intracerebrally with MVeGFP (200 $TCID_{50}$). Animals were monitored daily for clinical symptoms. In preliminary experiments we used the parental virus, Edtag (33), at similar titers. As early as 4 d.p.i. neurological illness, defined by ataxia and paralysis of the hind limbs, was observed (data not shown). We therefore sacrificed the MVeGFP-infected ani-

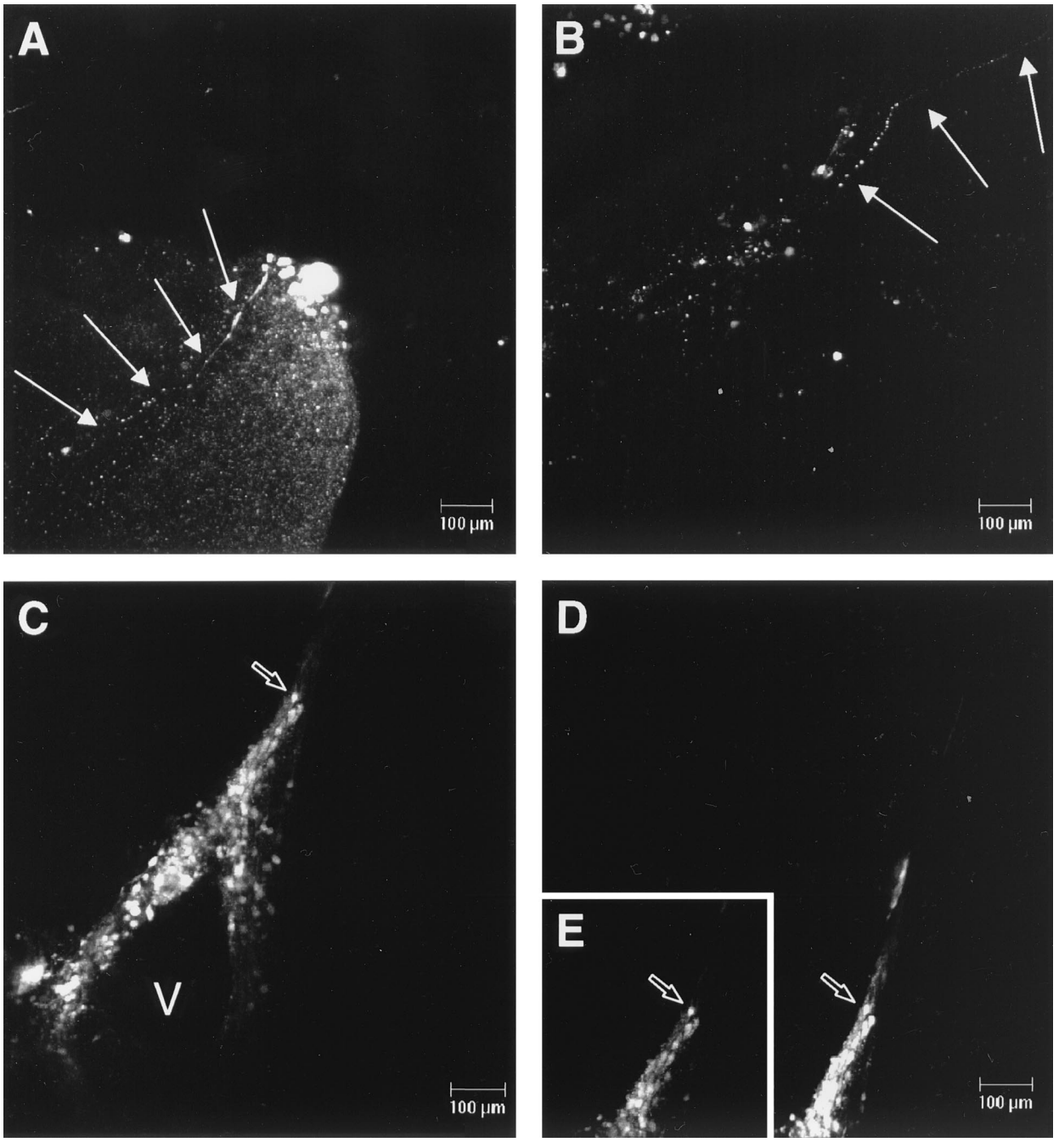

FIG. 3. Detection of EGFP autofluorescence in brain tissue from MVeGFP-infected Ifnar^{ko}-CD46Ge transgenic animals. Suckling animals were infected intracerebrally with MVeGFP (200 $TCID_{50}$). Animals were sacrificed 3 d.p.i., and brains were removed for observation by CSLM. (A) Focus of MVeGFP infection in the outer cortex of the brain. Arrows indicate a single process which extends from this focus into the brain parenchyma. (B) Neuronal process (arrowed) within an area of infection. (C) Infected ependymal and neuroblast cells surrounding a ventricle (V). This region of the brain tissue was observed after 6 h, and more cells were seen to be infected (D). Inset E is the equivalent region selected from C and aligned for comparison. An open arrow indicates the same cell (C, D, and E). Autofluorescent images were collected as before and are shown in "false" white.

mals at 3 d.p.i. to ascertain if EGFP autofluorescence could be detected at this time point in the infection and to observe the type of neural cells infected. Brains were removed and sectioned along the sagittal plane. Sections were placed in a petri dish containing serum-free medium under a 5% (vol/vol) CO_2 atmosphere. CSLM was used to collect image stacks through the tissue. Uninfected brains were also obtained to ascertain the overall level of background tissue-specific autofluorescence. A low level of tissue-specific autofluorescence was observed in these image stacks. This was, however, diffuse, and EGFP autofluorescence was clearly distinguishable in a number of discrete foci in the infected brain sections. Figure 3A shows a composite of 64 separate images of a typical focus of infection through 140.5 μm of brain tissue with spacing of approximately 2 μm. This focus of infection was located in the outer cortex of the brain. The parenchyma of the brain was

readily observed due to the low level of background tissue-specific autofluorescence. What became apparent upon generation of the composite images was the presence of long, EGFP-positive processes which extended into the tissue from the foci of infection (Fig. 3A and B, arrows). These processes were observed in other image stacks and were never observed in single images, as they would have had to be present entirely within one confocal plane. Therefore, the processes, which are transected by the individual focal planes of an image stack, appear as rows of dots. They were similar in appearance to those observed in the in vitro studies using the SH-SY-5Y and TMN cells. Figure 3B shows another example, this time within the tissue through an optical section of 150 μm. The process (arrow) can be seen to extend from an area of infection within the tissue.

The presence of EGFP within the MV genome allows the observation of CNS cells in very early stages of infection (14). EGFP autofluorescence was also observed in brain cells which did not have the morphology of neurons. Structures were observed which resembled a ventricle, as confirmed by light microscopy. Sixteen images were collected through a 21.9-μm optical section immediately after dissection (Fig. 3C). Based on the morphology and location of the EGFP-positive cells, we believe these are cells of the ependyma and surrounding neuroblasts. Hematoxylin and eosin (H&E) staining of sections from infected transgenic animals was used to confirm this. A projection was also observed to extend from the ventricle. Again based on morphology and with reference to H&E-stained sections, this is most likely the area of the brain which contains the developing neuroblasts. This area of the sections was observed 6 h later, and it was apparent that, during this time, more cells became positive (Fig. 3D). The inset (Fig. 3E), duplicated from Fig. 3C, shows the equivalent position in the tissue 6 h previously for comparison, and the same cell is indicated by an open arrow. The cells remained strongly positive for EGFP throughout the observation period, suggesting that MV replication was still occurring ex vivo.

We have not previously observed either infected ependymal or neuroblast cells in the mouse model of MV encephalitis using standard immunohistochemical techniques. Sections were therefore obtained from CAM/RB (rodent brain-adapted MV)-infected Ifnar^{ko}-CD46Ge animals at 6 d.p.i. to ascertain if it was possible to detect infected ependymal and neuroblast cells using this approach at this late stage of infection. Figure 4A shows cells of the ependyma and surrounding neuroblasts which are clearly positive for MV nucleocapsid antigen. Once again H&E staining was used to confirm the identity of the cells (Fig. 4B).

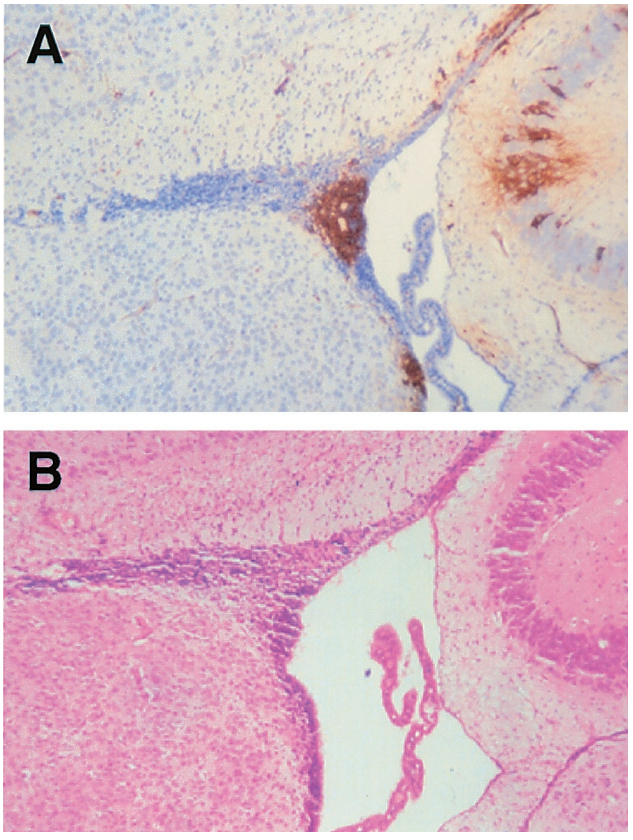

FIG. 4. Immunohistochemistry and H&E staining of brain sections from Ifnar^{ko}-CD46Ge suckling animals infected intracerebrally with the rodent brain-adapted virus CAM/RB. Sections were formalin fixed, and MV antigen was detected with an antinucleocapsid monoclonal antibody; positive staining appears brown. (A) Virus-infected neuroblasts and ependymal cells surrounding the ventricle. (B) H&E staining was used to confirm the identify of the infected cells. Magnification, ×100.

DISCUSSION

We have demonstrated here, both in vitro and in vivo, that MV is capable of utilizing neuronal processes to spread from cell to cell. This observation gives a clear indication of how discrete foci of infection may arise in the transgenic (Ifnar^{ko}-CD46Ge) model of MV CNS propagation. We have also shown appreciable levels of infection in cells of the ependyma and in the surrounding neuroblasts. This illustrates how MV establishes an infection in the transgenic model, and it is very possible that the same mechanisms may underlie MV spread in the more often used nontransgenic C57/BL/6 model. We have recently used this model to demonstrate that the H gene contains molecular determinants necessary for mouse neurovirulence (13) and are currently interested in determining if this observation is relevant to the human situation. In particular, we wish to elucidate how these alterations may affect virus spread in the CNS. It is apparent that the H gene permits MV to enter and spread within the rodent CNS, although no clear model exists for the mechanism or site of entry. Many viruses, such as canine parainfluenza virus and mumps virus, are known to infect the ependymal cells which line the ventricles of the brain (5, 45). We have used MVeGFP to demonstrate that many of the cells which surround the ventricles exhibit EGFP autofluorescence upon infection by the recombinant virus. Based on their location and morphological characteristics, we believe that these are ependymal and neuroblast cells. Infection of these two cell types by the rodent brain-adapted virus CAM/RB has also been confirmed by immunohistochemistry and H&E staining. It is known that MV can bind to murine ependymal cells (40). In previous studies using transgenic and nontransgenic systems, we and others have either failed to detect (13, 32) or observed only small numbers (31) of either infected ependymal cells or neuroblast cells using immunohistochemistry or in situ hybridization. Infected ependymal cells have been previously described in this model using higher titers of input virus (28). In this study a relatively small number of virus particles (200 $TCID_{50}$) were used for intracerebral infection, indicating that, following entry and replication, MVeGFP efficiently spreads to the neighboring cells surrounding the ventricle and thence to neuroblasts in the subependymal layer. At this stage many more of these cells were infected than neurons. These observations shed some light on how MV es-

tablishes an infection in the mouse model of encephalitis. However, it is difficult to imagine that they mimic the process by which MV enters the CNS in human infections. Nevertheless, they are relevant for the interpretation of data obtained in any subsequent studies which use rodent models of MV encephalitis.

One common observation made in all studies of MV infection, using both transgenic and rodent brain-adapted models, is the correlation between age of infection and extent of disease progression in the CNS (18, 23). This situation also exists in other experimental animal systems and humans (4, 34, 45). It is known that brain barriers mature postnatally, and it has been suggested, from studies on mumps virus, that this may be a major factor governing the overall progression of the infection in experimental animals (45). It has not, however, been established whether neuronal maturity has a role in slowing virus progression in the CNS. The contribution of the immune response to the protection of adult mice from CNS disease has been reported in a transgenic model, and it is clear that lymphocytes have an important role in modulating disease progression in adult animals (21). Only low levels of viral antigen were detected in brains of infected immunocompetent animals, whereas when the transgenic animal was back-crossed to T- and B-cell-deficient RAG-2^{-} knockout mice, significantly higher levels of infected neurons were observed.

These studies using MVeGFP virus therefore raise interesting questions in relation to the cell-to-cell spread of MV in particular and neurovirulent viruses in general in the CNS. The presence of CD46 is known to support virus entry (11, 30). In this study we have shown that MVeGFP, an Edmonston derivative, can infect murine cells at low levels. A previous study has also reported the infection of mouse neuroblastoma cells with the Edmonston strain of MV (17). It therefore seems that MV can infect cells in a CD46-independent manner, using an as yet unknown, possibly receptor-independent mechanism. It has been suggested that the virus spreads in the brain without budding (3, 22, 43), and the question of the precise role of CD46 in cell-to-cell spread in the CNS remains open. Recently Lawrence and colleagues have shown that cell contact but not CD46 expression is required for interneuronal spread (22). Undifferentiated and differentiated human neuroblastoma cells, primary murine neurons, and CD46-expressing primary murine neurons were used to demonstrate that MV spreads in the absence of budding. We have also differentiated the same neuroblastoma cell line and shown that the CAM/RB strain of the virus can enter CD46-negative differentiated neuroblastoma cells via CD46-positive neuroepithelial cells (27). It is therefore apparent that CD46 can support MV spread (28), although concomitant mechanisms may exist. Clearly rodent brain-adapted strains, such as CAM/RB, HNT, and Edtag-CAMH, can enter and spread in the absence of CD46. Currently it is most likely that a different receptor could be used to gain access to the CNS. Again, the role of this as yet uncharacterized receptor in the subsequent cell-to-cell spread of MV in the rodent CNS is unclear. Whether this is the same receptor(s) as for wild-type MV is not known.

In both SSPE and MV rodent models of encephalitis, little is known about the precise mechanism of MV spread in the CNS, although its anatomical distribution has suggested that the virus spreads transneuronally (2). This idea is substantiated by the frequent detection of antigen in neuronal processes in brain tissue from SSPE patients and the cell-associated nature of viruses isolated from SSPE cases (43). Viral antigen has also been detected in neuronal processes in infected rodents using immunohistochemistry and electron microscopy (13, 28, 32, 47). Axonal spread has been examined using the HNT virus in a study in which 8- to 10-week-old mice were injected in the right olfactory bulb (46). A low level of virus was detected in the brain in one of four animals 14 d.p.i. It was necessary to use mice which were deficient in the transporter associated with antigen presentation to achieve appreciable levels of infection in this model, and it is possible that this may be due to the age of the animals used. SSPE strains frequently have altered M proteins and mutations in the cytoplasmic tail of the F proteins (8, 39). Viruses which lack M protein and have alterations in the cytoplasmic tail of the F protein have been generated using the MV rescue system. These viruses lost acute pathogenicity but penetrated more deeply into the brain parenchyma of transgenic mice than standard MV, substantiating the notion that the ability to fuse efficiently rather than produce infectious virus modulates MV spread in the CNS (7). Recently it was proposed, based on the alignment of nucleocapsids near presynaptic membranes, that a novel mechanism of MV spread exists in mouse neurons which involves transynaptic spread (22). In this study we believe that we have demonstrated process-mediated spread, but at present, no evidence is available for the transmission of nucleocapsids through the synapse. In this context it should be considered that the glycoproteins of MV replicating in the brains of SSPE patients do maintain fusion functions, suggesting a role for the envelope proteins in cell-to-cell spread (9). Using MVeGFP, we have observed autofluorescence, and thereby detected virus indirectly, in neuronal processes which would be difficult to observe in embedded tissue sections at these early stages of infection. At this stage only small numbers of neurons were infected. This cell-to-cell, process-mediated spread is mirrored by the in vitro neuroblastoma model systems in which fusion is operative. It is clear from this study that the neurites which were generated upon differentiation of the TMN cells are utilized by MV to infect new cells and that MV makes use of these neurite-neurite connections to rapidly infect neighboring cells in the absence of virus budding. This confirms previous observations in other systems (22, 34). A similar situation occurs in the SH-SY-5Y infected cells. Interestingly, some cells remained uninfected even though they appeared to be in close proximity to the EGFP-positive and therefore virus-infected cells. This was also observed in recent studies using MVeGFP-infected astrocytoma cells (14).

This study has demonstrated the usefulness of MVeGFP for the study of MV cell-to-cell spread in vitro and in vivo. Utilization of neuronal processes in cell-to-cell spread has been demonstrated, but the precise mechanisms at the process-cell junctions are not yet clear. The high level of neuroblast cell infection has not been observed previously. This gives the first clear indication as to how an infection is established in the rodent models of MV encephalitis. The models developed in this study will aid in the dissection of the infection process of this neuropathogenic virus and may shed light on the precise mechanisms involved in transneuronal cell-to-cell spread. This is relevant for MV infections of the human CNS and may have wider implications for the study of other persistent neurotropic viruses. Alphaherpesviruses have been extensively used to study transneuronal spread and analyze neuronal circuitry (15, 44), and it may now be possible to use MVeGFP in similar studies.

ACKNOWLEDGMENTS

We thank Paula Haddock for excellent technical assistance and Roy Creighton for photographic work.

The Wellcome Trust (grant 047245) and the Swiss National Science Foundation (grant 31-45900.95) supported this work.

REFERENCES

1. **Agamanolis, D. P., J. S. Tan, and D. L. Parker.** 1979. Immunosuppressive measles encephalitis in a patient with a renal transplant. Arch. Neurol. **36:**686–690.
2. **Allen, I. V., S. McQuaid, J. McMahon, J. Kirk, and R. McConnell.** 1996. The significance of measles virus antigen and genome distribution in the CNS in SSPE for mechanisms of viral spread and demyelination. J. Neuropathol. Exp. Neurol. **55:**471–480.
3. **Baczko, K., U. G. Liebert, M. Billeter, R. Cattaneo, H. Budka, and V. ter Meulen.** 1986. Expression of defective measles virus genes in brain tissues of patients with subacute sclerosing panencephalitis. J. Virol. **59:**472–478.
4. **Baldwin, S., and R. J. Whitley.** 1989. Intrauterine herpes simplex virus infection. Teratology **39:**1–10.
5. **Baumgartner, W., S. Krakowka, and J. R. Gorham.** 1989. Canine parainfluenza virus-induced encephalitis in ferrets. J. Comp. Pathol. **100:**67–76.
6. **Blixenkrone-Moller, M., A. Bernard, A. Bencsik, N. Sixt, L. E. Diamond, J. S. Logan, and T. F. Wild.** 1998. Role of CD46 in measles virus infection in CD46 transgenic mice. Virology **249:**238–248.
7. **Cathomen, T., B. Mrkic, D. Spehner, R. Drillien, R. Naef, J. Pavlovic, A. Aguzzi, M. A. Billeter, and R. Cattaneo.** 1998. A matrix-less measles virus is infectious and elicits extensive cell fusion: consequences for propagation in the brain. EMBO J. **17:**3899–3908.
8. **Cattaneo, R., A. Schmid, D. Eschle, K. Baczko, V. ter Meulen, and M. A. Billeter.** 1988. Biased hypermutation and other genetic changes in defective measles viruses in human brain infections. Cell **55:**255–265.
9. **Cattaneo, R., and J. K. Rose.** 1993. Cell fusion by the envelope glycoproteins of persistent measles viruses which caused lethal human brain disease. J. Virol. **67:**1493–1502.
10. **Chan, S. P.** 1985. Induction of chronic measles encephalitis in C57BL/6 mice. J. Gen. Virol. **66:**2071–2076.
11. **Dorig, R. E., A. Marcil, A. Chopra, and C. D. Richardson.** 1993. The human CD46 molecule is a receptor for measles virus (Edmonston strain). Cell **75:**295–305.
12. **Dubois-Dalcq, M., T. S. Reese, M. Murphy, and D. Fuccillo.** 1976. Defective bud formation in human cells chronically infected with subacute sclerosing panencephalitis virus. J. Virol. **19:**579–593.
13. **Duprex, W. P., I. Duffy, S. McQuaid, L. Hamill, S. L. Cosby, M. A. Billeter, J. Schneider-Schaulies, V. ter Meulen, and B. K. Rima.** 1999. The H gene of rodent brain-adapted measles virus confers neurovirulence to the Edmonston vaccine strain. J. Virol. **73:**6916–6922.
14. **Duprex, W. P., S. McQuaid, L. Hangartner, M. A. Billeter, and B. K. Rima.** 1999. Observation of measles virus cell-to-cell spread in astrocytoma cells by using a green fluorescent protein-expressing recombinant virus. J. Virol. **73:**9568–9575.
15. **Enquist, L. W., P. J. Husak, B. W. Banfield, and G. A. Smith.** 1998. Infection and spread of alphaherpesviruses in the nervous system. Adv. Virus Res. **51:**237–347.
16. **Evlashev, A., E. Moyse, H. Valentin, O. Azocar, B. Trescol, J. C. Marie, C. Rabourdin-Combe, and B. Horvat.** 2000. Productive measles virus brain infection and apoptosis in CD46 transgenic mice. J. Virol. **74:**1373–1382.
17. **Gopas, J., D. Itzhaky, Y. Segev, S. Salzberg, B. Trink, N. Isakov, and B. Rager-Zisman.** 1992. Persistent measles virus infection enhances major histocompatibility complex class I expression and immunogenicity of murine neuroblastoma cells. Cancer Immunol. Immunother. **34:**313–320.
18. **Griffin, D. E., J. Mullinix, O. Narayan, and R. T. Johnson.** 1974. Age dependence of viral expression: comparative pathogenesis of two rodent-adapted strains of measles virus in mice. Infect. Immun. **9:**690–695.
19. **Hangartner, L.** 1997. M.Sc. thesis. University of Zürich, Zürich, Switzerland.
20. **Kobune, K., F. Kobune, K. Yamanouchi, K. Nagashima, Y. Yoshikawa, and M. Hayami.** 1983. Neurovirulence of rat brain-adapted measles virus. Jpn. J. Exp. Med. **53:**177–180.
21. **Lawrence, D. M., M. M. Vaughn, A. R. Belman, J. S. Cole, and G. F. Rall.** 1999. Immune response-mediated protection of adult but not neonatal mice from neuron-restricted measles virus infection and central nervous system disease. J. Virol. **73:**1795–1801.
22. **Lawrence, D. M., C. E. Patterson, T. L. Gales, J. L. D'Orazio, M. M. Vaughn, and G. F. Rall.** 2000. Measles virus spread between neurons requires cell contact but not CD46 expression, syncytium formation, or extracellular virus production. J. Virol. **74:**1908–1918.
23. **Liebert, U. G., and V. ter Meulen.** 1987. Virological aspects of measles virus-induced encephalomyelitis in Lewis and BN rats. J. Gen. Virol. **68:**1715–1722.
24. **Liebert, U. G., and D. Finke.** 1995. Measles virus infections in rodents. Curr. Top. Microbiol. Immunol. **191:**149–166.
25. **Manchester, M., D. S. Eto, and M. B. Oldstone.** 1999. Characterization of the inflammatory response during acute measles encephalitis in NSE-CD46 transgenic mice. J. Neuroimmunol. **96:**207–217.
26. **McQuaid, S., S. L. Cosby, K. Koffi, M. Honde, J. Kirk, and S. B. Lucas.** 1998. Distribution of measles virus in the central nervous system of HIV-seropositive children. Acta Neuropathol. (Berlin) **96:**637–642.
27. **McQuaid, S., S. Campbell, I. J. Wallace, J. Kirk, and S. L. Cosby.** 1998. Measles virus infection and replication in undifferentiated and differentiated human neuronal cells in culture. J. Virol. **72:**5245–5250.
28. **Mrkic, B., J. Pavlovic, T. Rulicke, P. Volpe, C. J. Buchholz, D. Hourcade, J. P. Atkinson, A. Aguzzi, and R. Cattaneo.** 1998. Measles virus spread and pathogenesis in genetically modified mice. J. Virol. **72:**7420–7427.
29. **Mrkic, B., B. Odermatt, M. A. Klein, M. A. Billeter, J. Pavlovic, and R. Cattaneo.** 2000. Lymphatic dissemination and comparative pathology of recombinant measles viruses in genetically modified mice. J. Virol. **74:**1364–1372.
30. **Naniche, D., G. Varior-Krishnan, F. Cervoni, T. F. Wild, B. Rossi, C. Rabourdin-Combe, and D. Gerlier.** 1993. Human membrane cofactor protein (CD46) acts as a cellular receptor for measles virus. J. Virol. **67:**6025–6032.
31. **Norrby, E., P. Swoveland, K. Kristensson, and K. P. Johnson.** 1980. Further studies on subacute encephalitis and hydrocephalus in hamsters caused by measles virus from persistently infected cell cultures. J. Med. Virol. **5:**109–116.
32. **Oldstone, M. B., H. Lewicki, D. Thomas, A. Tishon, S. Dales, J. Patterson, M. Manchester, D. Homann, D. Naniche, and A. Holz.** 1999. Measles virus infection in a transgenic model: virus-induced immunosuppression and central nervous system disease. Cell **98:**629–640.
33. **Radecke, F., P. Spielhofer, H. Schneider, K. Kaelin, M. Huber, C. Dotsch, G. Christiansen, and M. A. Billeter.** 1995. Rescue of measles viruses from cloned DNA. EMBO J. **14:**5773–5784.
34. **Rall, G. F., M. Manchester, L. R. Daniels, E. M. Callahan, A. R. Belman, and M. B. Oldstone.** 1997. A transgenic mouse model for measles virus infection of the brain. Proc. Natl. Acad. Sci. USA **94:**4659–4663.
35. **Rammohan, K. W., H. F. McFarland, W. J. Bellini, J. Gheuens, and D. E. McFarlin.** 1983. Antibody-mediated modification of encephalitis induced by hamster neurotropic measles virus. J. Infect. Dis. **147:**546–550.
36. **Reed, L. J., and H. Muench.** 1938. A simple method for estimating fifty percent endpoints. Am. J. Hyg. **27:**493–497.
37. **Rima, B. K., J. A. Earle, R. P. Yeo, L. Herlihy, K. Baczko, V. ter Meulen, J. Carabana, M. Caballero, M. L. Celma, and R. Fernandez-Munoz.** 1995. Temporal and geographical distribution of measles virus genotypes. J. Gen. Virol. **76:**1173–1180.
38. **Rima, B. K., J. A. Earle, K. Baczko, V. ter Meulen, U. G. Liebert, C. Carstens, J. Carabana, M. Caballero, M. L. Celma, and R. Fernandez-Munoz.** 1997. Sequence divergence of measles virus haemagglutinin during natural evolution and adaptation to cell culture. J. Gen. Virol. **78:**97–106.
39. **Schmid, A., P. Spielhofer, R. Cattaneo, K. Baczko, V. ter Meulen, and M. A. Billeter.** 1992. Subacute sclerosing panencephalitis is typically characterised by alterations in the fusion protein cytoplasmic domain of the persisting measles virus. Virology **188:**910–915.
40. **Tardieu, M., and H. L. Weiner.** 1982. Viral receptors on isolated murine and human ependymal cells. Science **215:**419–421.
41. **Taylor, M. J., E. Godfrey, K. Baczko, V. ter Meulen, T. F. Wild, and B. K. Rima.** 1991. Identification of several different lineages of measles virus. J. Gen. Virol. **72:**83–88.
42. **ter Meulen, V., J. R. Stephenson, and H. W. Kreth.** 1983. Subacute sclerosing panencephalitis, p. 105–159. *In* H. Fraenkel-Conrat and R. R. Wagner (ed.), Comprehensive virology. Plenum, New York, N.Y.
43. **ter Meulen, V.** 1997. Molecular and cellular aspects of measles virus persistence in the CNS. J. Neurovirol. **3:**S3–S5.
44. **Ugolini, G.** 1999. Transneuronal tracing with alpha-herpesviruses: a review of the methodology, p. 293–317. *In* M. G. Kaplitt and A. D. Loewy (ed.), Viral vectors: gene therapy and neuroscience applications. Academic Press Inc., San Diego, Calif.
45. **Uno, M., T. Takano, T. Yamano, and M. Shimada.** 1997. Age-dependent susceptibility in mumps-associated hydrocephalus: neuropathologic features and brain barriers. Acta Neuropathol. (Berlin) **94:**207–215.
46. **Urbanska, E. M., B. J. Chambers, H. G. Ljunggren, E. Norrby, and K. Kristensson.** 1997. Spread of measles virus through axonal pathways into limbic structures in the brain of TAP1$^{-/-}$ mice. J. Med. Virol. **52:**362–369.
47. **Van Pottelsberghe, C., K. W. Rammohan, H. F. McFarland, and M. Dubois-Dalcq.** 1979. Selective neuronal, dendritic, and postsynaptic localization of viral antigen in measles-infected mice. Lab. Investig. **40:**99–108.